Nuclear Physics B358 (1991) 497–523
North-Holland

THERMODYNAMIC BETHE ANSATZ FOR RSOS SCATTERING THEORIES

Al.B. ZAMOLODCHIKOV*

Departement de Physique de l'Ecole Normale Supérieure, 24 rue Lhomond, F-75231 Paris Cedex 05, France

Received 26 November 1990

Thermodynamic Bethe ansatz equations are suggested for RSOS scattering theories, which describe the scattering of kinks in the field theories, corresponding to the perturbations of the minimal CFT models $\mathcal{M}_p$ by relevant operators $\Phi_{(1,3)}$ with negative coupling constant. The equations turn to be of A_{p-2} type with a special choice of the mass terms. For the $\mathcal{M}_4$ case (tricritical Ising) the equations are studied numerically. This gives high precision data for the Casimir energy of the finite-volume system. The analytic continuation in the coupling constant results in reasonable numerical data for positive values of coupling. The data support the interpretation of the positive-coupling field theory as the trajectory flowing from the tricritical Ising fixed-point to the critical Ising one.

1. Introduction

Recently the thermodynamic Bethe ansatz (TBA) approach was used successfully to describe the finite-temperature effects for a number of relativistic factorized scattering theories (RFST) [1–6]. Conceptually, this approach simply specifies the original ideas of Yang and Yang [7] for the case of relativistic scattering (see refs. [2, 5] for detailed description of the TBA approach). Relativistic invariance, however, adds substantially to the interpretation possible. Suppose that some RFST is consistent, i.e. describes the scattering in some relativistic field theory (RFT) (note that this is not necessarily the case). The finite-temperature free energy, predicted by this scattering theory, can be interpreted as the Casimir energy of the finite-volume periodic system (currently we have in mind the euclidean field theory). On the other hand, in RFT the small volume behavior of the Casimir energy is described by the corresponding UV conformal field theory (CFT) [8]. Therefore, studying the high-temperature limit of the TBA equations, corresponding to some consistent RFST, one is able to identify the CFT, which governs the UV behavior of the background RFT, and also the integrable CFT

* Permanent address: Institute of Theoretical and Experimental Physics, B. Cheremushkinskaya 25, 117259, Moscow, USSR.

operator, drawing it out from the conformal fixed-point. This was the main line of study in refs. [1–5].

It seems important that in all the known relativistic examples the system of TBA equations has an impressively universal structure and can be related to the Dynkin diagram of some simply-laced Lie algebra $\mathcal{G}$ [2,5,6]. In particular, the number of equations coincides with the rank of the related algebra $\mathcal{G}$ and these equations are coupled in exactly the same way as the nodes of the corresponding Dynkin diagram are [6].

So far however, only diagonal (reflectionless) RFST's were explored in this way. In the present paper the TBA equations are proposed for non-diagonal scattering theories of kinks, which we call the $(\mathrm{RSOS})_n$; $n = 2,3,\ldots$ scattering theories. The $(\mathrm{RSOS})_n$ scattering theory is based on an n-fold degenerate vacuum-structure, the different vacua being associated with the nodes of the A_n Dynkin diagram. Denote the set of these nodes as $\mathscr{A}_n$. There are local (in the space dimension) field configurations, which link the vacua adjacent on the diagram. These configurations are the stable relativistic kinks of the same mass m. Transitions between different non-adjacent vacua can be arranged only by multikink states. This means that there are $2n-2$ different kinds of kinks (corresponding to the number $n-1$ of links on the A_n diagram), which can be denoted as $B_{\alpha\beta}$, where $\alpha,\beta \in \mathscr{A}_n$ are incident nodes of the A_n diagram. $B_{\alpha\beta}$ is the one-dimensional configuration with vacuum α to the left of the kink space-position and vacuum β to the right. The kink scattering is factorized and can be defined in terms of non-commuting symbols [9,10] $B_{\alpha\beta}(\theta)$, where θ denotes the kink rapidity. Corresponding to the two-kink scattering we have the following commutation relations

$$B_{\alpha\gamma}(\theta_1)B_{\gamma\beta}(\theta_2) = \sum_{\delta} S_{\alpha\beta}^{\gamma\delta}(\theta_1-\theta_2)B_{\alpha\delta}(\theta_2)B_{\delta\beta}(\theta_1), \tag{1.1}$$

where $\alpha,\beta,\gamma,\delta \in \mathscr{A}_n$ and the summation is over the vacua δ permitted by the adjacency condition. The pair-scattering amplitudes $S_{\alpha\beta}^{\gamma\delta}(\theta)$ are symmetric in both pairs of indices $S_{\alpha\beta}^{\gamma\delta}(\theta) = S_{\beta\gamma}^{\gamma\delta}(\theta) = S_{\alpha\beta}^{\delta\gamma}(\theta)$ and satisfy the crossing symmetry conditions

$$S_{\alpha\beta}^{\gamma\delta}(\theta) = S_{\gamma\delta}^{\alpha\beta}(i\pi-\theta), \tag{1.2}$$

and also the unitarity and factorization equations, which can be considered as the consistency conditions for the associative algebra of symbols $B_{\alpha\beta}(\theta)$. Essentially these amplitudes coincide with IRF (interaction round a face) Boltzmann weights of the exactly solvable RSOS (restricted solid-on-solid) lattice statistical models, discovered by Andrews et al. [11]. That is why we call these RFST's the $(\mathrm{RSOS})_n$ ones.

The simplest example (apart from the trivial $(\mathrm{RSOS})_2$ scattering theory, where kinks can be interpreted as the non-interacting massive particles) corresponds to

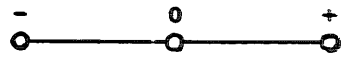

Fig. 1. Labeling of nodes on A_3 Dynkin diagram.

$n = 3$. In this case $\alpha = 0, \pm$ runs over the three nodes of A_3 diagram (fig. 1) and it is convenient to introduce new variable $\sigma = \pm$ to indicate the border vacua separately. There are four kinds of kinks $B_{0\sigma}$ and $B_{\sigma 0}$ with the scattering amplitudes

$$S_{00}^{\sigma\sigma'}(\theta) = F_{\sigma\sigma'}(\theta),$$

$$S_{\sigma\sigma'}^{00}(\theta) = G_{\sigma\sigma'}(\theta), \tag{1.3}$$

which are symmetric in their indices $F_{\sigma\sigma'}(\theta) = F_{\sigma'\sigma}(\theta)$, $G_{\sigma\sigma'}(\theta) = G_{\sigma'\sigma}(\theta)$, and satisfy the crossing symmetry

$$F_{\sigma\sigma'}(\theta) = G_{\sigma\sigma'}(i\pi - \theta), \tag{1.4}$$

unitarity

$$\sum_{\sigma = \pm} F_{\sigma_1\sigma}(\theta) F_{\sigma\sigma_2}(-\theta) = \delta_{\sigma_1\sigma_2},$$

$$G_{\sigma_1\sigma_2}(\theta) G_{\sigma_1\sigma_2}(-\theta) = 1, \tag{1.5}$$

and factorization constraints

$$\sum_{\sigma} F_{\sigma_1\sigma}(\theta) G_{\sigma_2\sigma}(\theta + \theta') F_{\sigma_3\sigma}(\theta') = G_{\sigma_2\sigma'}(\theta) F_{\sigma_1\sigma_3}(\theta + \theta') G_{\sigma_1\sigma_2}(\theta'). \tag{1.6}$$

They have the following explicit form

$$F_{\sigma\sigma'}(\theta) = \mathrm{e}^{-i\rho\theta} f_{\sigma\sigma'}(\theta)\sigma(\theta),$$

$$G_{\sigma\sigma'}(\theta) = \mathrm{e}^{i\rho\theta} g_{\sigma\sigma'}(\theta)\sigma(\theta), \tag{1.7}$$

where $\rho = (1/2\pi)\log 2$ is the constant necessary to provide the strict crossing symmetry (1.4) and $\sigma(\theta)$ is the meromorphic function, which solves the system of functional equations

$$\sigma(\theta) = \sigma(i\pi - \theta),$$

$$\sigma(\theta)\sigma(-\theta) = 1/\cosh(\theta/2), \tag{1.8}$$

and is free of zeros and poles in the strip $0 \leqslant \mathrm{Im}\,\theta \leqslant \pi$. The following integral

representation is most convenient for the purposes of the next section

$$\sigma(\theta) = [\cosh\theta/2]^{-1/2} \exp \frac{i}{4} \int_0^\infty \frac{\mathrm{d}t}{t} \frac{\sin \theta t/\pi}{\cosh^2 t/2} . \tag{1.9}$$

At last

$$\begin{aligned} f_{++}(\theta) &= f_{--}(\theta) = \cosh(\theta/4) , \\ f_{+-}(\theta) &= f_{-+}(\theta) = \sinh(\theta/4) , \\ g_{++}(\theta) &= g_{--}(\theta) = \cosh(\theta/4) - i \sinh(\theta/4) , \\ g_{+-}(\theta) &= g_{-+}(\theta) = \cosh(\theta/4) + i \sinh(\theta/4) , \end{aligned} \tag{1.10}$$

are entire $8i\pi$-periodic functions of θ. These explicit expressions will be of use below to derive the TBA equations for the $(\mathrm{RSOS})_3$ scattering theory. Explicit expressions for the general $(\mathrm{RSOS})_n$ scattering amplitudes can be easily derived from the weights of ref. [11].

In ref. [12] the $(\mathrm{RSOS})_{p-1}$ scattering theories were suggested as the on-mass-shell data of the RFT's, which arise as the perturbation of the unitary CFT minimal models $\mathcal{M}_p$ by the relevant scalar operator $\Phi = \Phi_{(1,3)}$ of dimension $\Delta = (p-1)/(p+1)$. These field theories (which we denote here by the symbol $\mathcal{M}\mathrm{A}_p^{(\pm)}$) can be defined by the perturbed action

$$A_{\mathcal{M}\mathrm{A}_p} = A_{\mathcal{M}_p} + \lambda \int \Phi(x)\, \mathrm{d}^2 x , \tag{1.11}$$

with real dimensional coupling constant λ. The physical content of the theory (1.11) looks essentially different for different signs of the coupling constant. The upper index near the symbol $\mathcal{M}\mathrm{A}_p^{(\pm)}$ was introduced above just to distinguish between these two different RFT's: $\mathcal{M}\mathrm{A}_p^{(+)}$ for $\lambda > 0$ and $\mathcal{M}\mathrm{A}_p^{(-)}$ for $\lambda < 0$. In ref. [12] it was argued that $\mathcal{M}\mathrm{A}_p^{(-)}$ is a massive field-theory with a finite correlation-length. On the other hand, as it was demonstrated in refs. [13, 14] on the basis of the perturbative renormalization group (RG), $\mathcal{M}\mathrm{A}_p^{(+)}$ is a massless RFT with two different CFT asymptotics in the ultraviolet (UV) and infrared (IR) limits. From the RG point of view it corresponds to the trajectory flowing from the $\mathcal{M}_p$ fixed point to the $\mathcal{M}_{p-1}$ one. The RG arguments are reliable only for p large, but this picture is presumably true for all $p > 3$ (the case $p = 3$ is definitely an exception, since $\mathcal{M}\mathrm{A}_3^{(+)} = \mathcal{M}\mathrm{A}_3^{(-)}$). Also it was observed in ref. [13] that this RG trajectory comes to the $\mathcal{M}_{p-1}$ fixed point mainly along the direction, defined by the irrelevant scalar operator $\Phi_{(3,1)}$ of dimension $\Delta_{(3,1)} = (p+2)/p$. This means, that in some not very strict sense one can consider $\mathcal{M}\mathrm{A}_p^{(+)}$ as the irrelevant perturbation of $\mathcal{M}_{p-1}$ by the corresponding field $\Phi_{(3,1)}$, i.e.

$$A_{\mathcal{M}\mathrm{A}_p^{(+)}} = A_{\mathcal{M}_{p-1}} + \gamma \int \Phi_{(3,1)}(x)\, \mathrm{d}^2 x + (\text{higher-dimension counterterms}) , \tag{1.12}$$

where γ is a coupling constant. This coupling has the dimension of an inverse power of the mass scale and therefore is small in the IR region. Note, that the IR perturbation theory, defined by the action (1.12), is non-renormalizable and we expect an infinite number of higher-dimension counterterms added in eq. (1.12). In the case of $\mathcal{M}A_4^{(+)}$ the IR CFT is $\mathcal{M}_3$ (the critical Ising), which has no operator $\Phi_{(3,1)}$ in the spectrum of local fields. Therefore the corresponding RG trajectory comes to the $\mathcal{M}_3$ fixed point along some other irrelevant operator. The most natural guess is the CFT field $\bar{T}T$ [15], i.e., the following IR action can be suggested

$$A_{\mathcal{M}A_4^{(+)}} = A_{\mathcal{M}_3} + g\int \bar{T}T(x)\,\mathrm{d}^2x + \text{counterterms}. \tag{1.13}$$

The coupling g here has the dimension of $(\text{mass})^{-2}$. This form of effective action is in agreement with the spontaneously broken supersymmetry of $\mathcal{M}A_4^{(+)}$, observed in ref. [15].

In ref. [16] A.B. Zamolodchikov argued perturbatively that $\mathcal{M}A_p$ is an integrable CFT and constructed explicitly some representatives of the higher integrals of motion. The local arguments of ref. [16] do not distinguish between positive and negative couplings and concern both $\mathcal{M}A_p^{(+)}$ and $\mathcal{M}A_p^{(-)}$. For massive $\mathcal{M}A_p^{(-)}$ the integrability leads to factorized scattering of massive excitations. It is for the $\mathcal{M}A_p^{(-)}$ model the $(\mathrm{RSOS})_{p-1}$ scattering theory was suggested as the RFST in ref. [12]. As for $\mathcal{M}A_p^{(+)}$, the consequences of integrability are not so clear. In any case the perturbation by $\Phi_{(3,1)}$ in the right-hand side of eq. (1.12), together with the higher counterterms, must be integrable. Using the same arguments as in ref. [16], one can conclude, that field $\Phi_{(3,1)}$ is indeed integrable to the first perturbative order and has the same set of integrals of motion, as the perturbation by $\Phi_{(1,3)}$ does. The same is true for field $\bar{T}T$ in action (1.13). In fact, infinitely many fields among the conformal descendants of $\Phi_{(1,3)}, \Phi_{(3,1)}$ and identity operator I can be found, which have the same common integrals of motion. This would mean, that perturbation by every mixture of these fields is formally integrable. It is not clear however, to what extent the first-order perturbative arguments are reliable in the case of non-renormalizable perturbation theory. Anyhow, we suppose that effective IR field-theory like (1.12) and (1.13) makes sense and can at least be used to produce asymptotic IR expansions, provided the counterterms are settled properly. Actions (1.12) and (1.13) definitely match the integrability at the first order. To preserve the integrability beyond this, special care must be taken about the higher counterterms.

It seems important to verify the above listed conjectures about $\mathcal{M}A_p^{(\pm)}$ non-perturbatively. In the present paper we try to use the TBA approach for this purpose, starting from the $(\mathrm{RSOS})_n$ scattering theories. Since these RFST's are non-diagonal, one must apply the higher-level Bethe ansatz technique [17] to derive the

Bethe ansatz equations. Instead of doing this we simply propose in sect. 2 a system of TBA integral equations, which seem to be rather suitable. These equations can be classified as A_{n-1} type in the ADE classification of ref. [6], since in this case $n-1$ integral equations are coupled exactly as the nodes of A_{n-1} Dynkin diagram. The analyses of the UV and IR limits of the equations proposed support both their interpretation as the TBA equations for the $(RSOS)_n$ scattering theories and their relevance for the $\mathcal{M}A^{(-)}_{n+1}$ field theory models. However, for the simplest case of $(RSOS)_3$, the direct derivation of the TBA system from the scattering theory described above is presented at the end of sect. 2.

To get more information, in sect. 3 the simplest example of the $(RSOS)_3$ related TBA equations is studied numerically. This results in a set of high-precision numerical data for the Casimir energy of the tricritical Ising model subject to the thermal perturbation by operator $\Phi_{(1,3)}$ of dimension 3/5 ($\mathcal{M}A^{(-)}_4$ model in the above notation). We are able to extract numerically the first several coefficients in the perturbative expansion of the Casimir energy and to compare them with the results of direct perturbative calculations. This gives in particular a numerical relation between the coupling λ in eq. (1.11) and the kink mass m. Also the analyticity of the Casimir energy in λ near $\lambda = 0$ is supported.

Supposing the Casimir energy to be analytic in λ, one can try to get some information about $\mathcal{M}A^{(+)}_n$ from the $\mathcal{M}A^{(-)}_n$ data by means of analytic continuation in the coupling. For the case of $\mathcal{M}A_4$ this is performed in sect. 4. Numerical analytic continuation of the high-precision TBA data results in a reasonable estimate of the $\mathcal{M}A^{(+)}_4$ Casimir energy. The bulk vacuum-energy and the IR central-charge are evaluated. The data support the $\mathcal{M}A^{(+)}_4$ field theory to be the flow from the tricritical Ising fixed-point to the critical Ising one [15]. Also we compare the IR behavior with the non-renormalizable perturbations of action (1.13). Although the data in the IR region are not reliable enough to perform a detailed analyses, we are able to verify the relevance of action (1.13) and to estimate roughly the relation between the IR coupling g and the UV coupling λ.

2. TBA equations for $(RSOS)_n$ scattering theories

In this section a system of TBA equations is proposed to describe the finite-temperature effects of the $(RSOS)_n$ scattering theory. We guess that this system can be obtained as the result of the higher-level Bethe ansatz, which takes account of the non-diagonal $(RSOS)_n$ kink scattering. Under the conjectures of ref. [12] this system describes also the Casimir energy $E(R)$ of the $\mathcal{M}A^{(-)}_{n+1}$ field-theory living on the space circle (the periodic boundary conditions are implied) of finite length R. The system is associated with the Dynkin diagram of Lie algebra A_{n-1}. It involves $n-1$ pseudoenergies $\varepsilon_a(\beta)$, $a = 1, 2, \ldots, n-1$ (real functions of rapidity β), which are attached to the nodes of the A_{n-1} diagram, as shown in fig. 2. Let l_{ab};

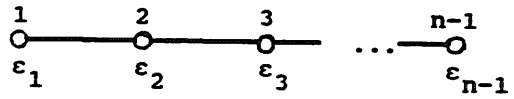

Fig. 2. Pseudo-energies ε_a, $a = 1, 2, \ldots, n-1$, which enter the TBA system (2.2), are attached to nodes of A_{n-1} diagram.

$a, b = 1, 2, \ldots, n-1$ be the incidence matrix of the A_{n-1} diagram, and

$$L_a(\beta) = \log(1 + e^{-\varepsilon_a(\beta)}). \tag{2.1}$$

The system reads as follows

$$-m_a R \cosh\beta + \varepsilon_a + \frac{1}{2\pi} \sum_b I_{ab} \varphi * L_b = 0. \tag{2.2}$$

Here

$$\varphi(\beta) = 1/\cosh\beta, \tag{2.3}$$

is the common kernel, and the star $*$ denotes the rapidity convolution

$$\varphi * L_a = \int_{-\infty}^{\infty} \varphi(\beta - \beta') L_a(\beta') \, d\beta' \tag{2.4}$$

The circle length R enters the equations only through the "mass term" $m_a \cosh\beta$. We choose the "mass spectrum" in the following way

$$m_1 = m, \qquad m_a = 0 \quad \text{for} \quad a = 2, 3, \ldots, n-1. \tag{2.5}$$

Provided $\varepsilon_a(\beta)$ solve system (2.2), the Casimir energy is given by

$$E(R) = -\sum_a \frac{m_a}{2\pi} \int \cosh\beta \, L_a(\beta) \, d\beta = -\frac{m}{2\pi} \int \cosh\beta \, L_1(\beta) \, d\beta. \tag{2.6}$$

Note, that eqs. (2.2) look precisely as if they would describe the system of $n-1$ different species of physical particles subject to a specially designed penetrable scattering. However, these particles except for the first one (corresponding to pseudo-energy $\varepsilon_1(\beta)$) have vanishing energies: $m_a \cosh\beta = 0$ for $a = 2, 3, \ldots, n-1$. It means that these pseudo-energies $\varepsilon_a(\beta)$, $a = 2, 3, \ldots, n-1$ correspond not to physical particles but rather to pseudoparticles, which are usual in the higher-level Bethe ansatz. Pseudoparticles carry no energy and their role is to arrange a suitable "color" structure of the Bethe ansatz wave function [17]. This interpretation will be supported shortly by the explicit calculation for a particular example.

Turning now to the analyses of system (2.2) consider first what one could expect for the low-temperature thermodynamics of the scattering theory $(RSOS)_n$. At low temperature $T = 1/R$ we have a dilute gas of far separated and slowly moving kinks with some vacuum structure in between. The kink interactions can be neglected completely. Nevertheless we have to allow for the statistics of the interkink vacua. The interkink vacuum "coloring" is governed by the $(RSOS)_n$ rules, i.e. it follows the A_n Dynkin diagram adjacency structure. Obviously, the corresponding specific (per kink) "color" entropy is determined by the largest eigenvalue of the A_n incidence matrix, which is known to be $2\cos(\pi/n+1)$. Therefore for $T \to 0$ we have

$$E(R) = -2\cos\frac{\pi}{n+1}\int\frac{m}{2\pi}\cosh\beta\, e^{-mR\cosh\beta}\,d\beta. \tag{2.7}$$

On the other hand, for $R = \infty$ $(T = 0)$ not all the pseudo-energies $\varepsilon_a(\beta)$ in eqs. (2.2) become infinite, as happens in the usual "massive" TBA equations. Pseudo-energy $\varepsilon_1(\beta)$ does, but the "massless" ones become finite rapidity-independent constants $\varepsilon_a(\infty)$. Denoting $y_a = \exp(-\varepsilon_a(\infty))$, $a = 2,3,\ldots,n-1$, we have the following equations for these constants

$$y_a^2 = \prod_{b=2}^{n-1}(1+y_b)^{\tilde{I}_{ab}}, \qquad a = 2,3,\ldots,n-1, \tag{2.8}$$

where $\tilde{I}_{ab}$; $a,b = 2,3,\ldots,n-1$ is the incidence matrix of the "restricted" A_{n-2} Dynkin diagram (the A_{n-1} diagram of fig. 2 without the first node). Therefore [2]

$$1 + y_a = \left[\frac{\sin(\pi a/(n+1))}{\sin(\pi/(n+1))}\right]^2. \tag{2.9}$$

Note, that this expression formally holds also for $y_1 = 0$. Substituting these constants in eqs. (2.2) as a zero-order low-temperature approximation, we find for the next iteration

$$\varepsilon_1(\beta) = mR\cosh\beta - \tfrac{1}{2}\log(1+y_2). \tag{2.10}$$

Under definition (2.6) this leads precisely to the $(RSOS)_n$ low-temperature estimation (2.7). In principle, the low-temperature iterations can be developed further and compared with the cluster expansion for the $(RSOS)_n$ kink gas. At present we skip this point.

For R finite the constants $\varepsilon_a(\infty)$ still persist as a limiting values of the functions $\varepsilon_a(\beta)$ as $\beta \to \pm\infty$. On the other hand, as $R \to 0$ (high-temperature limit) all the pseudo-energies tend to finite constants $\varepsilon_a(0)$ inside the "central region"

$-\log(1/mR) \ll \beta \ll \log(1/mR)$ [1–5]. The constants $x_a = \exp(-\varepsilon_a(0))$ now satisfy the system

$$x_a^2 = \prod_{b=1}^{n-1} (1+x_b)^{I_{ab}}, \qquad a = 1,2,\ldots,n-1 \tag{2.11}$$

with different solution

$$1+x_a = \left[\frac{\sin(\pi(a+1)/(n+2))}{\sin(\pi/(n+2))}\right]^2. \tag{2.12}$$

Performing the standard calculation [1–5, 11, 18, 19] we find for the leading $R \to 0$ asymptotics

$$E(R) \sim -\frac{1}{\pi R}\sum_{a=1}^{n-1}\left[\mathscr{L}\left(\frac{x_a}{1+x_a}\right) - \mathscr{L}\left(\frac{y_a}{1+y_a}\right)\right], \tag{2.13}$$

where $\mathscr{L}(x)$ is the Rogers dilogarithm function

$$\mathscr{L}(x) = -\tfrac{1}{2}\int_0^x \mathrm{d}t\left[\frac{\log t}{1-t} + \frac{\log(1-t)}{t}\right]. \tag{2.14}$$

With the dilogarithm sum rules [20] eq. (2.13) reduces to

$$E(R) \sim -\frac{\pi}{6R}\left(1 - \frac{6}{(n+1)(n+2)}\right). \tag{2.15}$$

This asymptotics is to be compared with the Casimir energy, predicted by conformal symmetry [8] for any unitary CFT with central charge c

$$E(R) = -\frac{\pi c}{6R}. \tag{2.16}$$

In particular, for $\mathscr{M}\mathrm{A}_{n+1}$ one would expect the leading UV behavior (2.16) with

$$c_n = 1 - \frac{6}{(n+1)(n+2)}, \tag{2.17}$$

in agreement with the above proposal of $\mathscr{M}\mathrm{A}_{n+1}^{(-)}$ as the background field theory.

Now turn to the bulk vacuum-energy contribution [1, 5], proportional to R. In the case under consideration this term is not the next to leading one in the $R \to 0$ expansion (except for the free-fermion case $n = 2$). Nevertheless, following the considerations of ref. [1] one again can express this contribution in terms of the

quantity $\tilde{L}_1^{(\mathrm{kink})}(k=i)$, where $\tilde{L}_a^{(\mathrm{kink})}(k)$ is the Fourier transform

$$\tilde{L}_a^{(\mathrm{kink})}(k)=\int L_a^{(\mathrm{kink})}(\beta)\mathrm{e}^{ik\beta}\,\mathrm{d}\beta, \tag{2.18}$$

of the "kink solution" (using the terminology of ref. [1]), i.e. the solution to the following modification of TBA equation (2.2)

$$-m_a R\,\mathrm{e}^{\beta}+\varepsilon_a^{(\mathrm{kink})}+\frac{1}{2\pi}\sum_b l_{ab}\varphi * L_b^{(\mathrm{kink})}=0. \tag{2.19}$$

Considering the analytic properties of the "kink solution" as a function of β (see below) one readily finds that the bulk-energy term vanishes for every odd n. For $n=3$ and $n=5$ this vanishing vacuum-energy is in nice agreement with the unbroken global supersymmetry and fractional supersymmetry, observed in the $(\mathrm{RSOS})_3$ and $(\mathrm{RSOS})_5$ scattering theories respectively [12]. We remark here that zero vacuum-energy implies that the specific heat is a regular function of the thermal coupling λ when it tends to the critical point $\lambda=0$ from below $\lambda\uparrow 0$. Of course, this does not mean that the specific heat is non-singular at $\lambda=0$; in sect. 4 we shall see that there is a singularity as $\lambda\downarrow 0$.

For n even, however, the same consideration leads formally to infinite vacuum-energy. In fact $\tilde{L}_1^{(\mathrm{kink})}(k)$ has a pole at $k=i$. As usual, this infinity signals the appearance of logarithmic contributions. The logarithm of this kind is well known in the Casimir energy of the free-fermion system (see e.g. [5]), which corresponds to $n=2$ in the $(\mathrm{RSOS})_n$ series. From the $\mathcal{M}\mathrm{A}_{n+1}^{(-)}$ point of view the nature of this logarithm is clear. Considering the perturbative expansion of the Casimir energy (see below) one observes the logarithmic divergence at order $(n+2)/2$, which gives the contribution

$$E_{\mathrm{pert}}^{((n+2)/2)}=\lambda^{(n+2)/2}R\bigl(C_1\log(R/\epsilon)+\mathrm{const.}\bigr), \tag{2.20}$$

where C_1 is some numerical (in principle calculable) constant, and ϵ is the UV cutoff (anybody who does not like infinite cutoffs is free to replace ϵ by an arbitrary dimensional normalization scale μ). Performing the subtraction necessary to adjust the perturbative UV structure to one predicted by TBA equations (2.2) (see eq. (2.22) below) one recovers the specific vacuum energy

$$\mathscr{E}_{\mathrm{vac}}=\lambda^{(n+2)/2}\bigl(-C_1\log(\epsilon\lambda^{(n+2)/4})+\mathrm{const.}\bigr). \tag{2.21}$$

Along with the predictable singular term $-\frac{1}{8}(n+2)^2C_1\lambda^{n/2}\log\lambda$ the vacuum expectation $\langle\Phi\rangle=(\partial/\partial\lambda)\mathscr{E}_{\mathrm{vac}}$ of the perturbing field $\Phi=\Phi_{(1,3)}$ contains indeterminate contributions non-singular in λ, which depend on the cutoff ϵ (or normal-

ization point μ). This ambiguity can be traced to the $(n/2)$th order resonance between the field Φ and the identity operator I [21]. The resonance leads to an indeterminate admixture of operator I into the perturbed field Φ, which cannot be fixed unless a normalization point is chosen. Naturally, this ambiguity does not affect the logarithmic specific-heat singularity (2.21) (note, that the power $(n+2)/2$ is integer for n even).

From the TBA point of view the observed logarithm can be treated as a result of the resonance between the $(n+2)/2$th regular term in the $R \to 0$ expansion (see below for the definition of regular terms) and the bulk-energy contribution. To estimate the coefficient before the logarithmic term one must adjust the above arguments to the resonance situation. For $R \to 0$ consider the central rapidity region $-\log(1/mR) \ll \beta \ll \log(1/mR)$. The functions $L_a(\beta)$ are nearly constant here, $L_a(\beta) = L_a(0) +$ corrections. Contrary to the non-resonance case, the term $Q_a \cosh\beta$ (with some constants Q_a) is permitted now among the corrections (see eq. (2.26) below). It is just this term that leads to logarithmic contribution in the integral (2.6). On the other hand a direct calculation fixes $Q_1 = mR/(n+2)$ (see appendix of ref. [27]). Therefore the logarithmic term in the Casimir energy (2.6) amounts

$$-\frac{m^2R}{2\pi}\frac{2}{n+2}(\log(mR) + C_2),$$

where C_2 is some unknown constant. One obtains the following form of the small R Casimir-energy expansion

$$E(R) = \frac{2\pi}{R}\left(-\frac{c_n}{12} - \frac{2}{n+2}\left(\frac{mR}{2\pi}\right)^2 \log(mR) + (\text{power terms})\right) \qquad (2.22)$$

We see again that the TBA is able to predict exactly the specific-heat singularity in terms of the correlation length m^{-1} [1,5].

To have more insight into the analytic structure of eqs. (2.2) we proceed as in ref. [6]. Note, that every solution to eqs. (2.2) satisfies also the functional relation

$$Y_a(\beta + i\pi)Y_a(\beta - i\pi) = \prod_b (1 + Y_b(\beta))^{I_{ab}}, \qquad a = 1,2,\ldots,n-1, \quad (2.23)$$

where functions

$$Y_a(\beta) = \exp(-\varepsilon_a(\beta)), \qquad (2.24)$$

were introduced. This functional equation has nearly the same form as the similar one related in ref. [6] to A_{n-1} penetrable scattering. Eq. (2.23) differs only in another step value in the left hand side and in that $Y_a(\beta)$ is now given by eq. (2.24)

instead of $\exp(\varepsilon_a(\beta))$ in ref. [6]. Nevertheless one can apply exactly the same arguments to conclude that $Y_a(\beta)$, $a = 1, 2, \ldots, n-1$ are entire functions in the whole β plane and satisfy the following periodicity

$$Y_a(\beta + i\pi(n+2)) = Y_a(\beta) \tag{2.25}$$

(note, that contrary to the example of ref. [6] we now have no symmetry $Y_a(\beta) = Y_{n-a}(\beta)$ in eqs. (2.2) and therefore the period is twice that quoted in ref. [6]). There is a regular expansion, convergent everywhere in the β-plane

$$Y_a(\beta) = \sum_{k \in \mathbb{Z}} Y_a^{(k)} e^{2k\beta/n+2}. \tag{2.26}$$

For the solution to eqs. (2.2) $Y_a^{(k)} = Y_a^{(-k)}$. The "kink solution" is regular also at $\beta = -\infty$, i.e. $Y_a^{(k)} = 0$ for $k < 0$. The form (2.26) suggests that for $R \to 0$ the Casimir energy (2.6) can be expanded in powers of $G = (mR)^{4/(n+2)}$ (except for single logarithmic term (2.22) at even n). For the scaling function $f(G) = (R/2\pi)E(R)$ we expect

$$f(G) = -\frac{c_n}{12} + \sum_{n=2}^{\infty} F_n G^n + (\text{log term (2.22) for even } n) \tag{2.27}$$

(along the lines of ref. [6] one can speculate that $F_1 = 0$ in expansion (2.27)).

Expansion (2.27) is to be compared with the Casimir-energy perturbative expansion [1, 5, 22], expected in $\mathcal{M}A_{n+1}$

$$f_{\text{pert}}(\lambda, R) = -\frac{c_n}{12} + \sum_n B_n t^n, \tag{2.28}$$

where $t = -2\pi\lambda(R/2\pi)^{4/(n+1)}$ is the dimensionless effective coupling and

$$B_n = -\frac{1}{(2\pi)^{n-1} n!} \int \langle \Phi(1,1)\Phi(x_1, \bar{x}_1) \ldots \Phi(x_{n-1}, \bar{x}_{n-1}) \rangle_c \prod_{i=1}^{n-1} \frac{d^2 x_i}{(x_i \bar{x}_i)^{1-\Delta}} \tag{2.29}$$

Here $\langle \Phi(1,1)\Phi(x_1, \bar{x}_1) \ldots \Phi(x_{n-1}, \bar{x}_{n-1}) \rangle_c$ is the connected infinite-plane n-point correlation function of CFT fields $\Phi = \Phi_{(1,3)}$ in $\mathcal{M}_{n+1}$ and $\Delta = n/(n+2)$ (for possible logarithmic divergences in integrals (2.29) one must keep in mind the metric $(R/2\pi)^2 \, dx \, d\bar{x}/x\bar{x}$ in the x-plane). For the purposes of sect. 3 we quote the first two terms in expansion (2.29), which can be carried out explicitly. Using the formulas [23]

$$\int \frac{d^2 x}{(x\bar{x})^{1-\Delta}[(1-x)(1-\bar{x})]^{2\Delta}} = \frac{\pi \gamma^2(\Delta)}{\gamma(2\Delta)}, \tag{2.30}$$

and

$$\int \frac{d^2x\, d^2y}{(x\bar{x}y\bar{y})^{1-\Delta}[(1-x)(1-\bar{x})(1-y)(1-\bar{y})(x-y)(\bar{x}-\bar{y})]^{\Delta}} = \frac{\pi^2\gamma^3(\Delta/2)}{2\gamma(3\Delta/2)}\,, \tag{2.31}$$

where $\gamma(x) = \Gamma(x)/\Gamma(1-x)$, we have

$$B_2 = -\frac{1}{4}\frac{\gamma^2(\Delta)}{\gamma(2\Delta)}\,,$$

$$B_3 = -\frac{\mathbb{C}_{\phi\phi\phi}}{48}\frac{\gamma^3}{2\gamma}\frac{(\Delta/2)}{(3\Delta/2)}\,. \tag{2.32}$$

Here $\mathbb{C}_{\phi\phi\phi}$ is the three-Φ structure constant in $\mathcal{M}_{n+1}$ [23]

$$\mathbb{C}_{\phi\phi\phi} = \frac{8\gamma(2\Delta)}{\Delta(1-3\Delta)\gamma^2(\Delta)}\left[\frac{\gamma(3(1-\Delta)/2)}{\gamma^3((1-\Delta)/2)}\right]^{1/2}. \tag{2.33}$$

The sign in eq. (2.33) is chosen so that $\mathbb{C}_{\phi\phi\phi}$ is positive. This choice of course is a matter normalization of the field Φ. It is for the choice (2.33) we have the interpretation described above of the coupling signs in $\mathcal{M}A_{n+1}$. In the first non-trivial example of $\mathcal{M}A_4$ we have

$$\left.\begin{aligned} B_2 &= \frac{25}{4\gamma(1/5)\gamma^2(2/5)} = 0.714401179\ldots \\ B_3 &= -\frac{1}{72}\left[\frac{\gamma^7(1/5)}{\gamma(2/5)}\right]^{1/2} = -1.385590503\ldots \end{aligned}\right\} \quad \text{for } \mathcal{M}A_4 \tag{2.34}$$

On the other hand in sect. 3 the TBA eqs. (2.2) are solved numerically for the simplest case of $(RSOS)_3$ scattering theory. We are able to extract numerically the first few coefficients F_n in expansion (2.27). Comparison with the numbers (2.34) supports the connection suggested above between eqs. (2.2) and $\mathcal{M}A^{(-)}_{n+1}$ field theories.

To end the section we present here the direct derivation of system (2.2) in the first non-trivial case $n = 3$, starting with the $(RSOS)_3$ scattering theory, which was described explicitly in sect. 1. Consider a state of N kinks in the periodic box of length L. L is supposed large as compared to the correlation length $R_c = m^{-1}$ and therefore the state can be described in terms of the kink wave function. Since the

kink scattering is factorized, this wave function is the Bethe one. As usual, the Bethe wave function is characterized by a set of N real rapidities $\beta_1, \beta_2, \ldots, \beta_N$, energy and momentum of the corresponding state being as follows

$$e(\beta_1, \ldots, \beta_N) = \sum_{k=1}^{N} m \cosh \beta_k ,$$

$$p(\beta_1, \ldots, \beta_N) = \sum_{k=1}^{N} m \sinh \beta_k . \tag{2.35}$$

An additional structure is related to non-trivial interkink vacuum "coloring". To allow for this introduce the color wave-function $\Psi^{\alpha_1 \ldots \alpha_N}$; $\alpha_1, \ldots, \alpha_N \in \mathscr{A}_n$. The colored Bethe wave-function can be conventionally represented as

$$\sum_{\alpha_1 \ldots \alpha_N \in \mathscr{A}_n} \Psi^{\alpha_1 \ldots \alpha_N} B_{\alpha_1 \alpha_2}(\beta_1) B_{\alpha_2 \alpha_3}(\beta_2) \ldots B_{\alpha_N \alpha_1}(\beta_N) \tag{2.36}$$

where $B_{\alpha\alpha'}(\beta)$ are the non-commuting symbols defined in sect. 1. Of course, the number of kinks must be even, $N = 2M$, to match the periodicity of the color wave-function and the $(\mathrm{RSOS})_n$ adjacency restrictions. Together with commutation relations (1.1) symbol (2.36) unambiguously determines the color structure of the Bethe wave-function for each space ordering of kinks.

If $L = \infty$ symbol (2.36) represents an allowed wave-function at every set of real rapidities $\beta_1, \ldots, \beta_N$. Keeping this set fixed one can consider the space Ψ of color wave-functions $\Psi^{\alpha_1 \ldots \alpha_N}$ as the space of states of a periodic N-point chain, which is a standard object in 2D lattice statistical mechanics (see e.g. ref. [24]). In standard way one defines the one-parameter family of commuting transfer-matrices $T(u) = T(u|\beta_1, \ldots, \beta_N)$ (parameterized by spectral parameter u) which act in space Ψ as follows (fig. 3)

$$(T(u)\Psi)^{\alpha_1 \ldots \alpha_N} = \sum_{\alpha'_1 \ldots \alpha'_N} S^{\alpha_1 \ldots \alpha_N}_{\alpha'_1 \ldots \alpha'_N}(u|\beta_1, \ldots, \beta_N) \Psi^{\alpha'_1 \ldots \alpha'_N} . \tag{2.37}$$

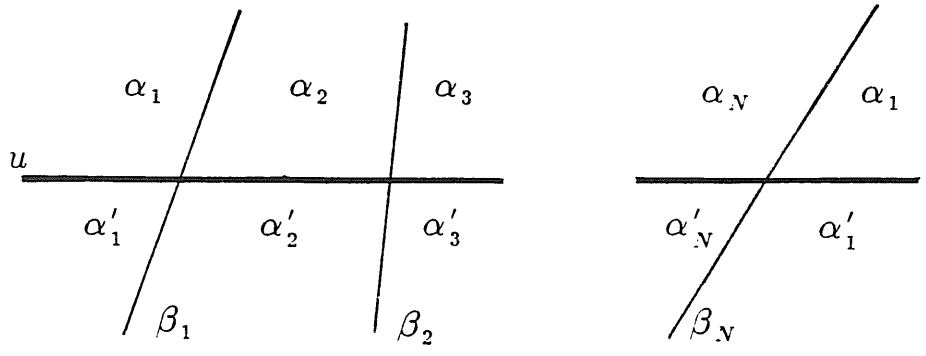

Fig. 3. $(\mathrm{RSOS})_n$ transfer-matrix.

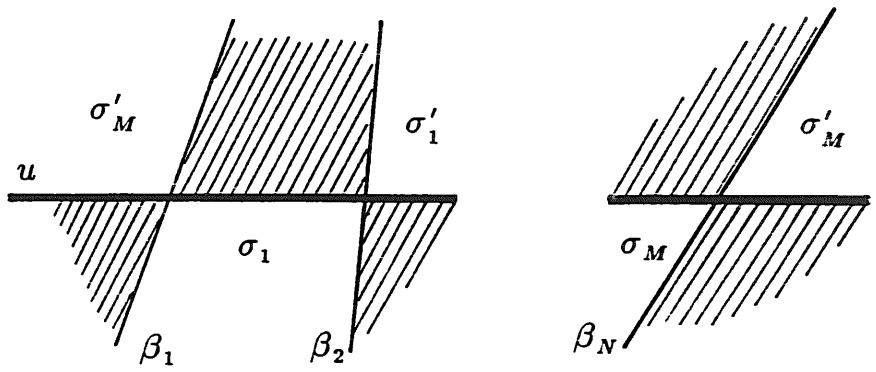

Fig. 4. Transfer-matrix of $(RSOS)_3$ scattering-theory. Dashed areas correspond to the vacuum $\alpha = 0$. Labeled areas carry $\alpha = \sigma = \pm$.

where the transfer-matrix entries

$$S^{\alpha_1 \dots \alpha_N}_{\alpha'_1 \dots \alpha'_N}(u|\beta_1, \dots, \beta_N) = S^{\alpha'_1 \alpha_2}_{\alpha_1 \alpha'_2}(u - \beta_1) S^{\alpha'_2 \alpha_3}_{\alpha_2 \alpha'_3}(u - \beta_2) \dots S^{\alpha'_N \alpha_1}_{\alpha_N \alpha'_1}(u - \beta_N) \quad (2.38)$$

are combinations of the $(RSOS)_n$ scattering amplitudes (1.1). The factorization of the kink scattering ensures the commutativity of the whole family $T(u)$, which therefore can be diagonalized simultaneously. The problem of finding the common eigenvectors $\Psi_l \in \Psi$, $l = 1, 2, \dots, \dim \Psi$ (which are independent of u) and the corresponding eigenvalues $\Lambda_l(u|\beta_1, \dots, \beta_N)$

$$T(u|\beta_1, \dots, \beta_N)\Psi_l = \Lambda_l(u|\beta_1, \dots, \beta_N)\Psi_l, \quad (2.39)$$

is a usual problem of integrable lattice-statistical-mechanics [24]. In fact, the transfer-matrix (2.37) is essentially an inhomogeneous version of the integrable RSOS model IRF transfer-matrix [11]. In the particular case $n = 3$ we mainly consider below it has a "staggered" structure described in fig. 4 and is (up to an overall factor) nothing but an inhomogeneous diagonal transfer-matrix of the critical Ising model.

Unlike the infinite-volume Bethe wave-function, in a finite box the set of rapidities $\beta_1, \dots, \beta_N$ is not arbitrary. It is restricted by the Bethe ansatz equations, which take account of the periodic boundary conditions. These can be settled formally by restricting the associative algebra of symbols $B_{\alpha\alpha'}(\beta)$ by the following cycle permutation relation

$$e^{imL \sinh \beta_1} B_{\alpha_1 \alpha_2}(\beta_1) B_{\alpha_2 \alpha_3}(\beta_2) \dots B_{\alpha_N \alpha_1}(\beta_N) = B_{\alpha_2 \alpha_3}(\beta_2) \dots B_{\alpha_N \alpha_1}(\beta_N) B_{\alpha_1 \alpha_2}(\beta_1). \quad (2.40)$$

It is straightforward to observe that the consistency of this additional restriction with the commutation relations (1.1) selects in the space of states (2.36) the states,

which satisfy Yang equations [17]

$$e^{imL\sinh\beta_k}\Lambda(\beta_k|\beta_1,\ldots,\beta_N)=1,\quad k=1,2,\ldots,N, \tag{2.41}$$

i.e. which are eigenvectors of the color transfer-matrix, the set $\beta_1,\ldots,\beta_N$ satisfying the system (2.41).

To write down eqs. (2.41) explicitly we have to find the eigenvalues of the transfer-matrix $T(u)$. At this point we turn to the simplest example, $n=3$, where the last problem coincides with the eigenvalue problem for the diagonal Ising transfer-matrix. The steps below are simply taken from ref. [24] with a minor modification allowing for the inhomogeneity of the chain.

Taking the explicit expression (1.7) for the $(RSOS)_3$ scattering amplitudes we first factor out the common multiplier

$$\Sigma(u|\beta_1,\ldots,\beta_N)=\exp\left(-i\rho\sum_{i=1}^{M}(\beta_{2i-1}-\beta_{2i})\right)\prod_{k=1}^{N}\sigma(u-\beta_k), \tag{2.42}$$

and define the reduced transfer-matrix $t(u|\beta_1,\ldots,\beta_N)$ by

$$T(u|\beta_1,\ldots,\beta_N)=\Sigma(u|\beta_1,\ldots,\beta_N)t(u|\beta_1,\ldots,\beta_N). \tag{2.43}$$

Then, the entries of the reduced transfer-matrix

$$t^{\sigma_1\ldots\sigma_M}_{\sigma'_1\ldots\sigma'_M}(u|\beta_1,\ldots,\beta_N)=g_{\sigma'_1\sigma_1}(u-\beta_1)f_{\sigma'_1\sigma_1}(u-\beta_2)\times g_{\sigma'_1\sigma_2}(u-\beta_3)f_{\sigma'_2\sigma_2}(u-\beta_4)$$
$$\ldots g_{\sigma'_{M-1}\sigma_M}(u-\beta_{N-1})f_{\sigma'_M\sigma_M}(u-\beta_N) \tag{2.44}$$

are entire $4i\pi$-periodic functions of the spectral parameter u. Considering the explicit form (1.10) of the functions $f_{\sigma\sigma'}(\beta)$ and $g_{\sigma\sigma'}(\beta)$ one finds that as $u\to\infty$ along the real axis every matrix element of $t(u)$ grows as $\exp(Mu/2)$ (or slower). The reduced eigenvalues $\lambda(u|\beta_1,\ldots,\lambda_N)=\Sigma^{-1}(u|\beta_1,\ldots,\lambda_N)\Lambda(u|\beta_1,\ldots,\lambda_N)$ exhibit the same analytic properties (as functions of the spectral parameter). Moreover, due to obvious invariance of amplitudes (1.10) under the simultaneous reversion of both spins (we use here the Ising model terms and refer to variables σ as the spins), every eigenstate has a definite parity $r=\pm$ under the simultaneous reversion of all the spins in the state. The corresponding operation in Ψ is denoted as R. It is easy to check that

$$t(u+2\pi i)=(-)^M Rt(u), \tag{2.45}$$

and therefore an eigenvalue of parity r satisfies

$$\lambda(u+2i\pi|\beta_1,\ldots,\beta_N)=(-)^M r\lambda(u|\beta_1,\ldots,\beta_N). \tag{2.46}$$

This means that the u-dependence of every eigenvalue λ is as follows

$$\lambda(u) = A\prod_{i=1}^{M} \sinh\frac{u-x_i}{2} \quad \text{for} \quad R\text{-even states},$$

$$\lambda(u) = A\prod_{i=1}^{M-1} \sinh\frac{u-x_i}{2} \quad \text{for} \quad R\text{-odd states}, \tag{2.47}$$

where A is some u-independent constant and x_i, $i = 1,2,\ldots,M$ (or $M-1$) are complex numbers (eigenvalue zeroes), which always can be put inside the strip $-\pi < \operatorname{Im} x_i \leqslant \pi$. Their positions depend on the eigenstate and also on the set of rapidities $\beta_1,\ldots,\beta_N$.

Next, exploiting the factorization and unitarity (1.5), (1.6) of the kink scattering-amplitudes, one readily recovers the following "inversion relation" [24]

$$t(u)t(u+i\pi) = \prod_{k=1}^{N} \cosh\frac{u-\beta_k}{2} + R\prod_{k=1}^{N} \sinh\frac{u-\beta_k}{2}, \tag{2.48}$$

which results in the functional equation for the entire eigenvalue functions $\lambda(u)$

$$\lambda(u)\lambda(u+i\pi) = \prod_{k=1}^{N} \cosh\frac{u-\beta_k}{2} + r\prod_{k=1}^{N} \sinh\frac{u-\beta_k}{2}, \tag{2.49}$$

where r is the parity of the state we are considering. Taking the representation (2.47) one concludes that M eigenvalue zeroes x_i ($M-1$ in the odd case) can be found among $N = 2M$ (respectively $N-2$) zeroes of the right-hand side of eq. (2.49). The last form in the strip $-\pi < \operatorname{Im} x_i \leqslant \pi$ a set of complex-conjugate pairs $x_i^{(+)} = y_i \pm \frac{1}{2}i\pi$ (fig. 5) (we remind that all the rapidities β_k are supposed real), where the set of numbers y_i, $i = 1,2,\ldots,M$ ($M-1$ in the odd case) includes all

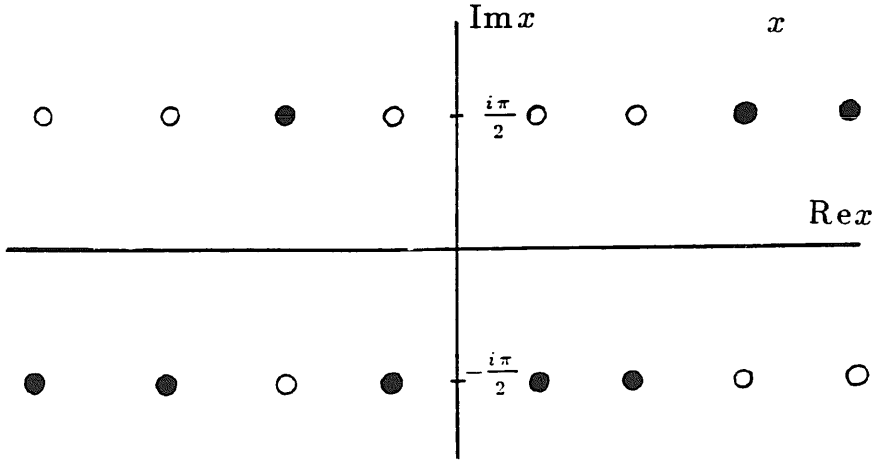

Fig. 5. Zeroes of the r.h.s. of eq. (2.49) are examplified as circles. Full circles are actual zeroes of a particular eigenvalue.

the finite real solutions to the following equation

$$\prod_{k=1}^{N} \frac{\sinh\left(\frac{y_i-\beta_k}{2}+\frac{i\pi}{4}\right)}{\sinh\left(\frac{y_i-\beta_k}{2}-\frac{i\pi}{4}\right)} = r(-)^M . \tag{2.50}$$

One can pick one zero from each pair to collect the set of zeroes necessary for the eigenvalue function. In the odd case there are exactly 2^{M-1} possible choices, corresponding to 2^{M-1} odd eigenstates. In the even case there is in fact one additional restriction on the choice of actual eigenvalue zeroes, which reduces the number of allowed distributions from 2^M to 2^{M-1} [24]. We shall not discuss here this subtlety because it obviously has no thermodynamic consequences. Note, that once the set $\beta_1,\ldots,\beta_N$ is chosen the positions of the zeroes we have to pick out from are prescribed by eq. (2.50) and do not depend on the actual eigenstate. Surely this simplification is a reflection of the free-fermion nature of the Ising-model space of states and is not expected to persist for systems with interacting excitations.

Turn now to the thermodynamic limit $N \to \infty$, which corresponds to $L \to \infty$. As it is usual in TBA [7], one introduces the rapidity density of kink states $\rho(\beta)$ and the actual density of kinks $\rho_1(\beta)$. For the density of kinks fixed introduce also the densities $P_\pm(y)$ of eigenvalue zeroes located respectively at $x = y \pm \frac{1}{2}i\pi$. The joint density $P(y) = P_+(y) + P_-(y)$ is obviously the density of solutions to eq. (2.50). Differentiating the last equation with respect to y one finds in the thermodynamic limit

$$2\pi P(y) = \int \frac{\rho_1(\beta)\,\mathrm{d}\beta}{\cosh(y-\beta)} . \tag{2.51}$$

Another relation, which determines the density of kink states, follows from the Yang equation (2.41)

$$2\pi\rho(\beta) = mL\cosh\beta + \int \varphi_{\sigma}(\beta-\beta')\rho_1(\beta')\,\mathrm{d}\beta' + \frac{1}{2}\int \frac{P_+(y)-P_-(y)}{\cosh(\beta-y)}\,\mathrm{d}y . \tag{2.52}$$

Here

$$\varphi_{\sigma}(\beta) = \frac{\partial}{\partial\beta}\,\mathrm{Im}\log\sigma(\beta) = \frac{1}{4}\int \frac{\mathrm{e}^{ik\beta}}{\cosh^2(\pi k/2)}\,\mathrm{d}k , \tag{2.53}$$

comes from eq. (1.9). In the derivation of eq. (2.52) only the phases of the

scattering amplitudes are taken into account. Due to relation (2.51) the contributions of the corresponding absolute values cancel out completely. Together with (2.51) eq. (2.52) gives the following set

$$2\pi\rho(\beta) = mL\cosh\beta + \int \frac{P_+(y)\,dy}{\cosh(\beta - y)},$$

$$2\pi P(y) = \int \frac{\rho_1(\beta)\,d\beta}{\cosh(y - \beta)}. \tag{2.54}$$

The zeroes distribution entropy and the rapidity distribution entropy are

$$\mathscr{S}_{\text{zeroes}} = \int dy(P\log P - P_+\log P_+ - P\ \log P_-),$$

$$\mathscr{S}_{\text{kink}} = \int dy(\rho\log\rho - \rho_1\log\rho_1 - (\rho - \rho_1)\log(\rho - \rho_1)). \tag{2.55}$$

Introduce pseudo-energies ε_1 and ε_2 as

$$\frac{\rho_1}{\rho} = \frac{e^{-\varepsilon_1}}{1 + e^{-\varepsilon_1}}, \qquad \frac{P_+}{P} = \frac{e^{-\varepsilon_2}}{1 + e^{-\varepsilon_2}}. \tag{2.56}$$

With the total energy of the kink system $m\int\cosh\beta\,\rho_1(\beta)d\beta$ and restrictions (2.54) the thermodynamic equilibrium at temperature $T = 1/R$ leads precisely to the TBA equations (2.2) (for $n = 3$) and the Casimir energy as in eq. (2.6).

3. Numerical results for the $(RSOS)_3$ system

For $n = 3$ eqs. (2.2) form a system of two coupled integral equations. This system was solved numerically by an iterative procedure. The scaling function

$$f(R) = -\frac{mR}{(2\pi)^2}\int\cosh\beta\log(1 + e^{-\varepsilon_1(\beta)})\,d\beta, \tag{3.1}$$

is presented in table 1 up to 15 decimal digits accuracy. In fig. 6 $f(R)$ is plotted against the dimensionless parameter

$$G = (mR)^{4/5}. \tag{3.2}$$

For G close to zero the curve appears as a regular function at $G = 0$ with the G-expansion starting with $-\frac{7}{120} + F_2G^2 + \ldots$ and without any vacuum-energy

TABLE 1
Casimir energy scaling-function for $\mathcal{A}(A_4^{(1)})$ field theory

mR	f(mR)	mR	f(mR)
6.50	-3.62942701038764E-4	1.20	-3.36671739751558E-2
6.40	-3.98300299046595E-4	1.10	-3.58920181164612E-2
6.30	-4.37056009241474E-4	1.00	-3.81826520224492E-2
6.20	-4.79530117936897E-4	0.98	-3.86475403001348E-2
6.10	-5.26072204564086E-4	0.96	-3.91144024943628E-2
6.00	-5.77063686093473E-4	0.94	-3.95831062194533E-2
5.90	-6.32920560792635E-4	0.92	-4.00535124404785E-2
5.80	-6.94096363151517E-4	0.90	-4.05254752073521E-2
5.70	-7.61085341761691E-4	0.88	-4.09988413735313E-2
5.60	-8.34425871697840E-4	0.86	-4.14734502978640E-2
5.50	-9.14704112467607E-4	0.84	-4.19491335279299E-2
5.40	-1.00255792181231E-3	0.82	-4.24257144630172E-2
5.30	-1.09868103448672E-3	0.80	-4.29030079946316E-2
5.20	-1.20382751353986E-3	0.78	-4.33808201221578E-2
5.10	-1.31881647946475E-3	0.76	-4.38589475409694E-2
5.00	-1.44453711977143E-3	0.74	-4.43371771999053E-2
4.90	-1.58195397793332E-3	0.72	-4.48152858245923E-2
4.80	-1.73211251611120E-3	0.70	-4.52930394025762E-2
4.70	-1.89614494039516E-3	0.68	-4.57701926256177E-2
4.60	-2.07527627032334E-3	0.66	-4.62464882837880E-2
4.50	-2.27083062590429E-3	0.64	-4.67216566051482E-2
4.40	-2.48423769502835E-3	0.62	-4.71954145337726E-2
4.30	-2.71703933170496E-3	0.60	-4.76674649376542E-2
4.20	-2.97089622067840E-3	0.58	-4.81374957365485E-2
4.10	-3.24759452628650E-3	0.56	-4.86051789380188E-2
4.00	-3.54905242253358E-3	0.54	-4.90701695677459E-2
3.90	-3.87732637681318E-3	0.52	-4.95321044774681E-2
3.80	-4.23461703107225E-3	0.50	-4.99906010105646E-2
3.70	-4.62327449096729E-3	0.48	-5.04452555011151E-2
3.60	-5.04580279522181E-3	0.46	-5.08956415769991E-2
3.50	-5.50486329345500E-3	0.44	-5.13413082309066E-2
3.40	-6.00327661073273E-3	0.42	-5.17817776145402E-2
3.30	-6.54402282056297E-3	0.40	-5.22165425001566E-2
3.20	-7.13023938465809E-3	0.38	-5.26450633389918E-2
3.10	-7.76521634726961E-3	0.36	-5.30667648267240E-2
3.00	-8.45238819416373E-3	0.34	-5.34810318600376E-2
2.90	-9.19532170143022E-3	0.32	-5.38872047326924E-2
2.80	-9.99769900759752E-3	0.30	-5.42845733699835E-2
2.70	-1.08632950444859E-2	0.28	-5.46723703303926E-2
2.60	-1.17959483586023E-2	0.26	-5.50497622020086E-2
2.50	-1.27995242465434E-2	0.24	-5.54158388716128E-2
2.40	-1.38778690157088E-2	0.22	-5.57695999170663E-2
2.30	-1.50347540662238E-2	0.20	-5.61099370179049E-2
2.20	-1.62738083712166E-2	0.18	-5.64356107022112E-2
2.10	-1.75984378088776E-2	0.16	-5.67452187727388E-2
2.00	-1.90117296668970E-2	0.14	-5.70371520230755E-2
1.90	-2.05163404894845E-2	0.12	-5.73095295855773E-2
1.80	-2.21143652539727E-2	0.10	-5.75600995990835E-2
1.70	-2.38071856221290E-2	0.08	-5.77860759534626E-2
1.60	-2.55952946683956E-2	0.06	-5.79838436315460E-2
1.50	-2.74780949754398E-2	0.04	-5.81483464702709E-2
1.40	-2.94536661984790E-2	0.02	-5.82714627978236E-2
1.30	-3.15184969609686E-2	0.00	-5.83333333333333E-2

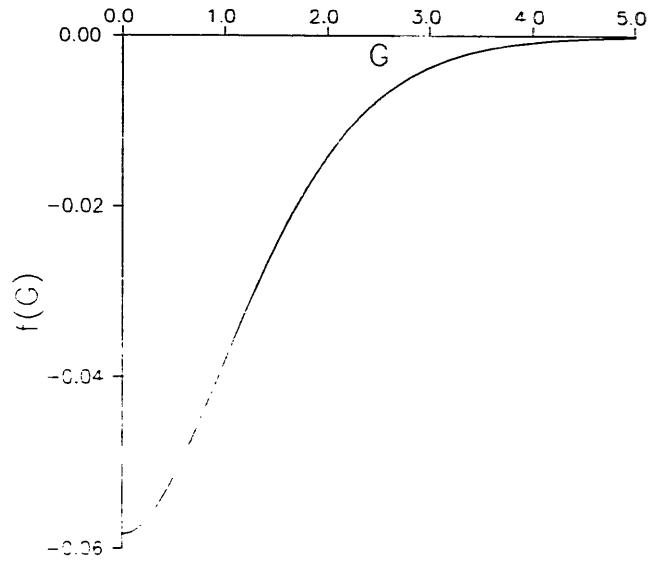

Fig. 6. Casimir-energy scaling-function vs. $G = (mR)^{4/5}$.

term, which would behave in this example as $G^{5/2}$. More careful analyses of the data in the interval $0 \leqslant G \leqslant 0.5$ reliably shows that this analytic structure is indeed the case and permits to recover numerically the first several coefficients F_n in expansion (2.27). The numbers are quoted in table 2. Comparing the first coefficient F_2 with the corresponding term in perturbative expansion (2.34) we are able to find the following numerical relation between the $\mathcal{M}A_4^{(-)}$ coupling constant λ and the kink mass m

$$\lambda = (-0.310148596\ldots)m^{4/5}. \tag{3.3}$$

With this number in hand one can transform the rest of the coefficients of table 2

TABLE 2
The first several coefficients F_n in expansion (2.27)

n	F_n
2	$3.2946543241(1) \times 10^{-2}$
3	$-1.372260104(1) \times 10^{-2}$
4	$3.681163(1) \times 10^{-4}$
5	$5.111(1) \times 10^{-4}$
6	$8.42(1) \times 10^{-5}$
7	$-2.38(1) \times 10^{-5}$
8	$-1.3(1) \times 10^{-5}$

to perturbative ones B_n [eq. (2.28)]. In particular, the value of F_3 gives

$$B_3 = -1.38559050(1), \tag{3.4}$$

(the digit in brackets here and below is the uncertainty in the last digit quoted) in agreement with the direct perturbative result of eq. (2.34).

4. From tricritical Ising to critical Ising by analytic continuation

Suppose the analytic behavior of the scaling function $F(G)$ observed numerically in the previous section is correct. Then it is natural to use the high precision data at $G \geqslant 0$ for analytic continuation into the negative G region. Under the connection observed in sect. 2 between the G-expansion and the perturbative series in coupling constant λ, we expect this negative G region to describe the Casimir energy of the positive coupling field theory $\mathcal{M}A_4^{(+)}$.

The rational extrapolation technique was used. Based upon $N = 18, \ldots, 26$ positive G data points inside the interval $0 \leqslant G < 0.5$ the N-point Thiele fraction [25] was constructed, which represents the diagonal $[N/2, N/2]$ N-point Padé approximant. For actual extrapolation we used the fractions with $N = 22$ or 24, which give the most stable numbers in the interval $-4 < G < 0$. The result is plotted in fig. 7 together with few points representing the "exact" TBA data for $G > 0$.

The most interesting thing to explore is the behavior of the extrapolation data as $G \to -\infty$. Since we believe them to estimate the Casimir-energy scaling-function of $\mathcal{M}A_4^{(+)}$, this limit corresponds to the IR region, where the dimensionless circle length

$$r = (-G)^{5/4} \tag{4.1}$$

becomes large. The leading term one would expect here is the bulk vacuum-energy. In the scaling function it appears as a rise with r as $r^2 = (-G)^{5/2}$ and is definitely non-zero, as one can observe in fig. 7. The supersymmetry of the action (1.11) for $n = 4$ is broken spontaneously at $\lambda > 0$ and therefore it is realized non-linearly. In fig. 8 the function $f(r)/r^2$ is plotted against $1/r^2$. Apart from a small region of $1/r^2 < 0.015$ close to the origin, where the curve goes up fast (we attribute this effect to a fault with the rational extrapolation at $-G$ large) the data are well fitted by the straight line

$$f(r) = Ar^2 + C, \tag{4.2}$$

where

$$A = 0.03980(1), \qquad B = -0.042(1). \tag{4.3}$$

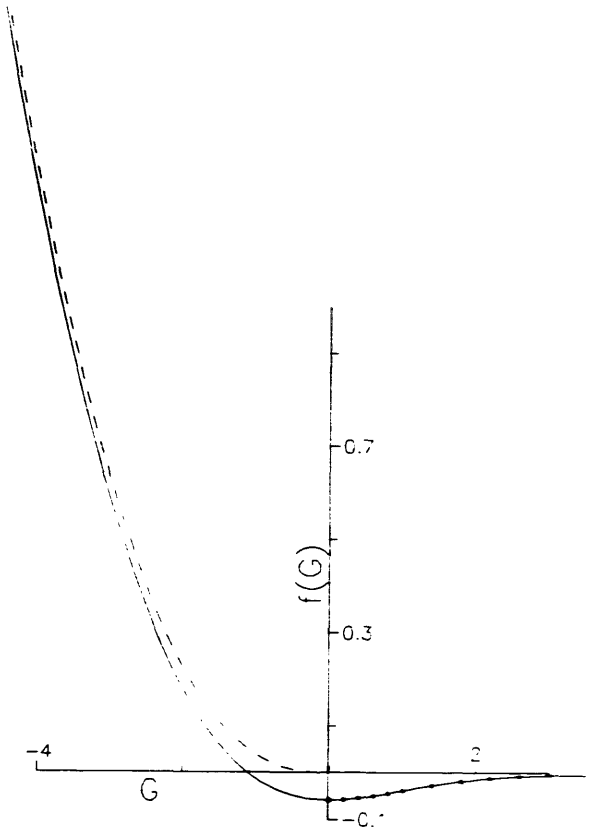

Fig. 7. Padé extrapolation from $0 \leqslant G < 0.5$. Solid curve – extrapolation data. * – "exact" TBA points at $G > 0$. Dashed curve – bulk vacuum-energy $0.03980(-G)^{5/2}$.

The first number corresponds to the bulk vacuum-energy in $\mathcal{M}A_4^{(+)}$

$$\mathcal{E}_{\text{vac}} = 2\pi m^2 A\,. \tag{4.4}$$

It is interesting to note, that numerically A coincides (within the accuracy quoted in (4.3)) with $1/8\pi$. The second number B is in agreement with $-1/24$ (this is $-c/12$ at $c = 1/2$), i.e. what one would expect in the IR region of the trajectory flowing to the critical Ising fixed point.

Unfortunately, in the infrared region $r \to \infty$ the extrapolation data (see table 3 and fig. 9) are not precise enough to say something definite about the next IR corrections. These corrections are closely related to the scalar irrelevant-operator, which attracts the trajectory to the IR fixed-point. In the case under consideration the guess of operator $\bar{T}T \sim :\bar{\psi}\partial\bar{\psi}\psi\partial\psi:$ (where $\psi, \bar{\psi}$ are the Ising massless free-fermion fields), as in eq. (1.13), seems most natural [15]. First, it has the lowest dimension among the irrelevant operators permitted by symmetry arguments. Second, one can readily repeat the dimension-counting arguments of ref. [16] to convince oneself that the operator $\bar{T}T$ is integrable to first perturbative order (this holds not only for the critical Ising model, but in fact for every CFT). However, in

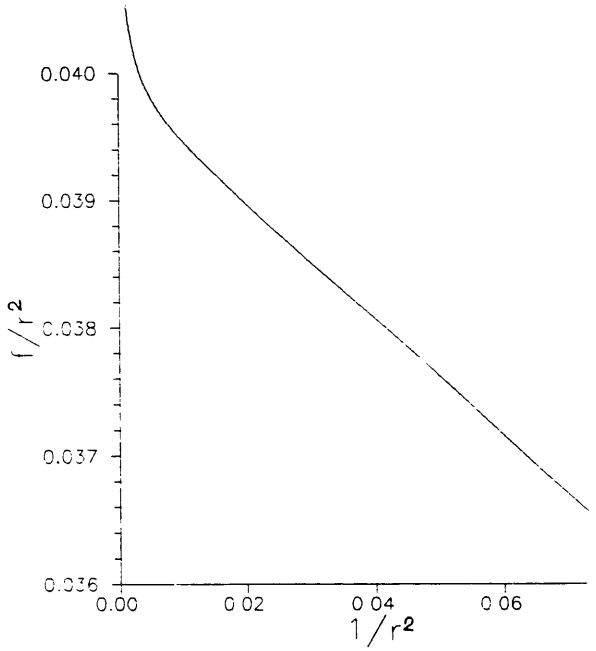

Fig. 8. $f(r)/r^2$ against $1/r^2$; $r = (-G)^{5/4}$.

the case of irrelevant perturbation the first-order check does not prove the integrability, unlike the relevant case, where the first-order perturbation (or at least finitely many perturbative terms) typically completely determines the structure of higher integrals of motion [16]. Dimensional counting allows in fact an infinite number of higher-dimension CFT operators to appear in any conservation low beyond the first $\bar{T}T$ perturbation. Nevertheless we expect, that the higher-dimension counterterms in the action (1.13) always can be picked so as to provide a real integrability.

TABLE 3
Function $U(G) = f(G) - 0.0398(-G)^{5/4}$ is tabulated vs G

G	$U(G)$	G	$U(G)$
−3.0	−4.398E-2	−1.0	−5.15010E-2
−2.8	−4.433E-2	−0.9	−5.22282E-2
−2.6	−4.473E-2	−0.8	−5.29904E-2
−2.4	−4.5190E-2	−0.7	−5.37815E-2
−2.2	−4.5730E-2	−0.6	−5.45918E-2
−2.0	−4.6364E-2	−0.5	−5.54068E-2
−1.8	−4.7107E-2	−0.4	−5.62055E-2
−1.6	−4.7978E-2	−0.3	−5.69573E-2
−1.4	−4.89924E-2	−0.2	−5.76170E-2
−1.2	−5.01650E-2	−0.1	−5.81159E-2
		0.0	−5.83333E-2

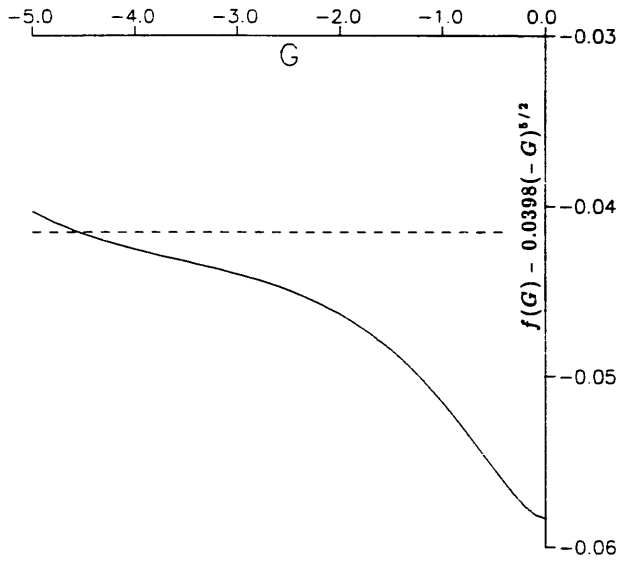

Fig. 9. Extrapolation data without vacuum energy contribution, i.e. $f(r) - 0.03980r^2$ (solid curve). Dashed line corresponds to expected infrared limit $-1/24$.

Starting from the action (1.13) one can develop formally the following IR perturbative expansion of the Casimir-energy scaling-function

$$f(R) = -\frac{c}{12} - 2\pi \sum_{n=1}^{\infty} \frac{(-\alpha/2\pi)^n}{n!} \int |\langle \tau(1)\tau(z_2)\dots\tau(z_n)\rangle_c|^2 \prod_{i=2}^{n} |z_i|^2 \, d^2 z_i \quad (4.5)$$

where $\alpha = (2\pi)^3 g/R^2$ and $\langle \tau(z_1)\dots\tau(z_n)\rangle_c$ is the connected infinite-plane correlation function of n operators $\tau(z) = T(z) - (c/24z^2)I$. Here and in eq. (4.5) c is the central charge in the infrared CFT ($c = 1/2$ in the actual case). The first two terms read explicitly

$$f(R) = -\frac{c}{12} + \left(\frac{c}{24}\right)^2 \alpha - \left(\frac{c}{24}\right)^3 \alpha^2 + O(\alpha^3) \quad (4.6)$$

The one-loop integral contributing at order α^2 develops UV-divergences of orders g^2/ϵ^6 and g^2/ϵ^2 (where ϵ is the UV cutoff length), which can be attributed respectively to a cutoff-dependent shift in the bulk vacuum-energy and to a perturbative renormalization (diffeomorphism) of the coupling g

$$g_R = g + \text{const.} \frac{g^2}{\epsilon^2} + \dots, \quad (4.7)$$

where g_R is the renormalized coupling constant. The next term of order α^3 in expansion (4.6) is ambiguous since at this order the first possible counterterm $(\bar{T}T)^2$ in the r.h.s. of eq. (1.13) becomes to contribute with an undetermined coupling constant.

Nevertheless the terms present in eq. (4.6) predict the following asymptotic expansion

$$f(r) = Ar^2 + C + \frac{C_1}{r^2} + \frac{C_2}{r^4} + \frac{C_3}{r^6} + \dots , \tag{4.8}$$

where the bulk vacuum energy A is not determined directly by the perturbation theory of the action (1.13), $C = -1/24$ and

$$C_1 = Q/48^2 , \qquad C_2 = Q^2/48^3 . \tag{4.9}$$

Q is the following R-independent combination

$$Q = \alpha r^2 = (4630.36318\dots)\, g\lambda^{5/2} \tag{4.10}$$

(the numerical result (3.3) was used to compute the number in the r.h.s.), which depends on the relation between UV and IR coupling constants of $\mathcal{M}A_4^{(+)}$.

As a result of a somewhat more careful analyses of the extrapolation data (including the analyses of a small deviation from the linear dependence in fig. 8) we obtained the following numerical estimation of the next term in expansion (4.8)

$$C_1 = -0.04 \pm 0.01 , \tag{4.11}$$

from which the relation follows

$$g = (-2.0 \pm 0.5)\lambda^{-5/2} . \tag{4.12}$$

Unfortunately the precision here is not enough even to be sure that this correction follows exactly the behavior (4.8). Also we are not able to extract the next term of order α^2, not to talk about the α^3 correction, which would provide information about the first counterterm in the effective action (1.13).

5. Conclusions

We presented some analytic and numerical evidences supporting both the interpretation of the $(RSOS)_n$ scattering theories as the on-mass-shell data of $\mathcal{M}A_{n+1}^{(-)}$ field theory models and the system (2.2) as the corresponding system of TBA equations.

The numerical analytic continuation of TBA data, corresponding to $\mathcal{M}A_4^{(-)}$ model, is in agreement with the interpretation of $\mathcal{M}A_4^{(+)}$ as the RG trajectory

flowing from the tricritical Ising fixed-point to the critical Ising one. Also they are in support, though much less certain, of (1.3) as an effective IR action of $\mathcal{M}A_4^{(\tau)}$.

I am grateful to V.A. Fateev for stimulating discussions.

Notes added

(i) After the paper was finished, I received the preprint by Itoyama and Moxhay [26], where the TBA system (2.2) is suggested, although with a much different interpretation.

(ii) It turns possible to describe the Casimir energy in $\mathcal{M}A_{n+1}^{(+)}$ field theories directly by a kind of massless TBA system, modifying slightly system (2.2) [27].

Note added in proof

T. Klassen and E. Melzer pointed out to me that the number quoted in eq. (3.3) is accidentally off by a factor of $(2\pi)^{2/5}$. The correct relation is $\lambda = (-0.148695516\ldots)m^{4/5}$. The other numbers quoted in the paper are unchanged. I would like to thank T. Klassen and E. Melzer for this and many other relevant remarks.

References

[1] Al.B. Zamolodchikov, Nucl. Phys. B342 (1990) 695
[2] T.R. Klassen and E. Melzer, Nucl. Phys. B338 (1990) 485
[3] M.J. Martins, Phys. Lett. B240 (1990) 404
[4] P. Christe and M.J. Martins, Mod. Phys. Lett. A5 (1990) 2189
[5] T.R. Klassen and E. Melzer, Nucl. Phys. B350 (1991) 635
[6] Al.B. Zamolodchikov, Phys. Lett. B253 (1991) 391
[7] C.N. Yang and C.P. Yang, J. Math. Phys. 10 (1969) 1115
[8] H.W. Blote, J.L. Cardy and M.P. Nightingale, Phys. Rev. Lett. 56 (1986) 742
[9] A.B. Zamolodchikov and Al.B. Zamolodchikov, Ann. Phys. (N.Y.) 120 (1979) 253
[10] P.P. Kulish, Proc. LOMI Sem. 109 (1981) 83
[11] G.E. Andrews, R.J. Baxter and P.J. Forrester, J. Stat. Phys. 35 (1984) 193
[12] A.B. Zamolodchikov, Landau Institute preprint (1989)
[13] A.B. Zamolodchikov, Sov. J. Nucl. Phys. 46 (1987) 1090
[14] A. Ludwig and J. Cardy, Nucl. Phys. B285 [FS19] (1987) 687
[15] D.A. Kastor, E.J. Martinec and S.H. Shenker, Nucl. Phys. B316 (1989) 590
[16] A.B. Zamolodchikov, Kiev preprint ITP 87-65P (1987)
[17] C.N. Yang, Phys. Rev. Lett. 19 (1967) 1312
[18] V.V. Bazhanov and N.Yu. Reshetikhin, Serpukhov preprint N27 (1987)
[19] V.V. Bazhanov, A.N. Kirillov and N.Yu. Reshetikhin, Pisma ZhETF 46 (1987) 500
[20] L. Lewin, Polylogarithms and associated functions (North-Holland, Amsterdam, 1981)
[21] Al.B. Zamolodchikov, Nucl. Phys. B348 (1991) 619
[22] H. Saleur and C. Itzykson, J. Stat. Phys. 48 (1987) 449
[23] Vl.S. Dotsenko and V.A. Fateev, Nucl. Phys. B251 [FS13] (1985) 691
[24] R.J. Baxter, Exactly solved models in statistical mechanics (Academic Press, New York, 1982)
[25] T.N. Thiele, Interpolationsrechnung (Teubner, Leipzig, 1909)
[26] H. Itoyama and P. Moxhay, Phys. Rev. Lett. 65 (1990) 2102
[27] Al.B. Zamolodchikov, preprint ENS-LPS-327 (1991)